Design of a Compact SRR Loaded Polarization-Independent Wideband Metamaterial Rasorber with a Narrow Transmission Window

Abhinav Kumar[1, 3], Gobinda Sen[2, *], and Jayanta Ghosh[3]

[1]*Department of ECE, Bhagalpur College of Engineering, Bhagalpur, India*
[2]*Department of ECE, Institute of Engineering & Management, Kolkata, India*
[3]*Department of ECE, National Institute of Technology, Patna, India*

ABSTRACT: This work presents a new compact split-ring resonator (SRR)-loaded rasorber to achieve narrow in-band transmission while maintaining broad absorption over a wide frequency range. The unit cell on the top layer is made up of four 150-ohm lumped resistors and four modified split ring resonators that are capable of absorbing a wide range of frequencies. The bottom FSS layer comprises a multilayer cascaded structure where top and bottom most metal layers are inductive grids, and the middle-sandwiched layer is a folded square ring structure. This design serves as a band-pass filter, allowing in-band transmission frequencies to pass through and also serving as a ground plane for out-of-band frequencies. The proposed rasorber exhibits an absorption bandwidth of 124% for frequency band starting from 2.5 GHz to 9.5 GHz, which covers mostly ISM and Satellite communication bands. The rasorber also acts as a transparent structure with insertion loss of 1.3 dB at the IOT band of 4.8 GHz. The novelty of the rasorber lies in achieving a very narrow transmission bandwidth with sharp roll off and is well suitable for radome applications having high selectivity. The innovation in this design comes from its combination of wide out-of-band absorption, narrow in-band transmission, high angular stability up to 50° for oblique incidence, and a dual-polarized response. The study looked at polarization behavior, surface current distribution, and other important parameters to figure out how well the rasorber worked. The equivalent circuit response of the proposed rasorber is compared with simulated one to get more circuit level understanding. Our results indicate that the electrical equivalent circuit design closely aligns with the simulated data. The proposed rasorber is suitable for secure communication in defense, as a super-stratum on an antenna, with reduced RCS and stealth characteristics.

1. INTRODUCTION

Frequency-Selective Rasorbers (FSRs) are generally two-layer structures that pass the in-band frequency window when both layers have infinite impedance and absorb the out-of-band absorption window, when the top layer's frequency selective surface (FSS) impedance matches the free space impedance, and the bottom layer behaves as a ground plane. By passing the desired band for a specific purpose, it creates a shield around the object, reducing the likelihood of radar detection. Thus, they are opaque for out-of-band frequency regime and transparent for in-band transmission window. It is employed in military aircraft and ships to safeguard against hostile radar. They can also be employed in recreational vehicles such as watercraft and automobiles to reduce the likelihood of accidents caused by collisions with other objects [1]. A lot of FSSs have been used as hybrid Radomes in antenna systems to lower the radar cross section (RCS), improve radiation performance, and stop the interference between systems [2–5]. They are employed in Radomes structures, and as a result, they are referred to as Rasorbers (Radomes and Absorbers) or FSR [6, 7]. Radomes are structures that serve as protective enclosures for radar systems and other devices. Their design

is centered on the reduction of radar detectability and the minimization of signal interference. These structures typically consist of materials that either reflect or block radio frequency signals, which lowers the emissions and makes them harder for radar to pick up [8]. Radomes are currently receiving increased attention as a result of their ability to transmit in-band signals and absorb out-of-band messages. They are composed of two layers, with the upper layer serving as an absorption layer and the lower layer as a signal transmission layer. The top layer is equipped with a lumped resistor, resistive sheet, or ink to achieve a broad spectrum of absorption [9]. A band-pass selective transmission can be designed by cutting a proper slot in the bottom layer [10].

The FSR is a specialized structure that combines absorber and filter functions, utilizing a dual-layer approach to achieve unique transmission characteristics. Initially, rasorbers were designed with the transmission band preceding the absorption band, using band-pass geometry below a resistive sheet. This design faced challenges due to the inherently lossy nature of resistive sheets [11]. Researchers have employed a variety of methods to introduce parallel resonance into frequency selective rasorber (FSR) designs. Making parallel LC slots in metallic dipole elements that are loaded with chip resistors is one

---

* Corresponding author: Gobinda Sen (gobinda.dets@gmail.com).

FIGURE 1. Absorption and transmission phenomena of the rasorber.

way to do it [12–14]; this creates parallel resonance. Another approach involves placing lumped LC elements in parallel with the resistive element, a technique that can create parallel resonance but may also lead to high insertion loss due to parasitic resistance from the lumped components [15]. A related technique uses two series RLC circuits connected in parallel, with resistors bypassed in the passband by the series LC circuits. This setup makes a way for energy to move around the resistive parts while transmission is happening, which helps keep the passband's efficiency [16]. Another variation uses a parallel LC circuit inside the resistive sheet. This is done by adding lossless slot-type frequency selective surfaces (FSSs) and lumped resistors to other slot resonators of different lengths to control the absorption band [17]. This combination of techniques allows for greater flexibility in rasorber design and helps to mitigate the challenges posed by lossy resistive sheets. Different techniques [18–24] can only absorb the signal from any one side of the passband. To absorb the signal on both sides of the passband, the rasorber with in-band communication is required, meaning that there is a transmission window between two absorption bands on either side [25, 26].

This study has developed a polarization-insensitive, high-angle-independent, wide-out-of-band, and narrow-in-band transmission window rasorber. It is a unique type of FSS that can assimilate incoming signals and transmit a specific frequency band simultaneously. The proposed rasorber is composed of two layers. The top layer is employed for wideband absorption, while the bottom layer is positioned at an appropriate distance from the top layer to allow the in-band signal to pass through. We introduced parallel (L_5-C_5) resonators in the bottom layer to transmit the in-band signal losslessly. Our objective was to create a narrow, in-band transmission window. To achieve this, two rectangular slots were placed above and below the parallel L_5-C_5 resonator, which introduced series (L_3-C_3) and (L_4-C_4) resonators, as illustrated in Figure 12. The top layer is loaded with lumped resistors to increase the bandwidth of the out-of-band absorption from 2.5 to 9.5 GHz. The parallel L_5-C_5 resonator, which is introduced in the lower layer, is responsible for the transmission band at 4.8 GHz with an insertion loss of 1.3 dB. Furthermore, Advance Design System (ADS) software is employed to develop an equivalent circuit model for both in-band and out-of-band operations. The proposed rasorber has been investigated for its angular stability, surface current density, polarization insensitivity, and design parameters. Finally, the simulated results and effective equivalent circuit model were compared, and they were found to be in excellent agreement. This validates the concept and design of the proposed rasorber. The proposed rasorber has the potential to be implemented in defense and other critical

installations for secure communication, ground planes for the antenna, reduced RCS, and stealth characteristics.

2. THEORETICAL BACKGROUND

Rasorber generally comprises two layers. It is the job of the top lossy layer to absorb the signal. The bottom lossless layer, on the other hand, will work as a band-pass filter to send in-band signals and a ground plane for the out-of-band absorption window. The overall frequency regime of the rasorber can be divided into three parts, i.e., lower absorption band (f_1), transmission window (f_2), and upper absorption band (f_3), as shown in Figure 1.

For an ideal absorber, the reflection coefficient ($S_{11} = 0$), and transmission coefficient ($S_{21} = 0$), absorptivity can be calculated by Eq. (1) [18], but the rasorber phenomenon is different from the absorber.

$$A(\omega) = 1 - |S_{11}|^2 - |S_{21}|^2 \qquad (1)$$

where $A(\omega)$, $|s_{11}|^2$, $|s_{21}|^2$ are absorption, reflected power, and transmitted power, respectively.

For the rasorber at f_1 and f_3, $S_{11} = 0$ and $S_{21} = 0$ should be zero, and at f_2, S_{21} should be unity. The proposed rasorber has been carefully designed to achieve these phenomena, as illustrated in Figure 2. i.e., when the impedance of the top layer is matched to the free space impedance and zero for the bottom layer, the structure behaves as an absorber. To get a transmission window, the impedance of both layers should be infinity.
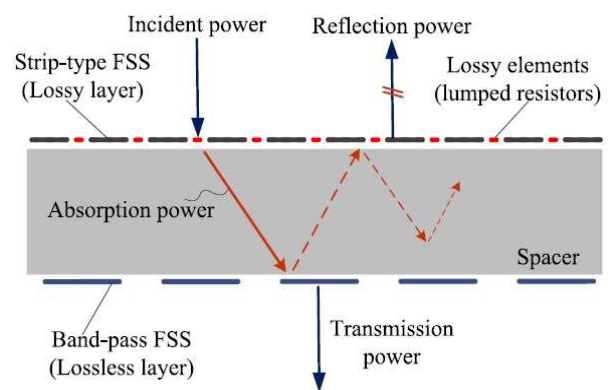
FIGURE 2. Absorption and transmission phenomena based on cavity model.

3. UNIT CELL GEOMETRY

The proposed rasorber unit cell geometry comprises two layers. In this particular design, we employed the principle of a quarter-wave transmission line that is terminated with a short circuit to achieve specific performance characteristics. This
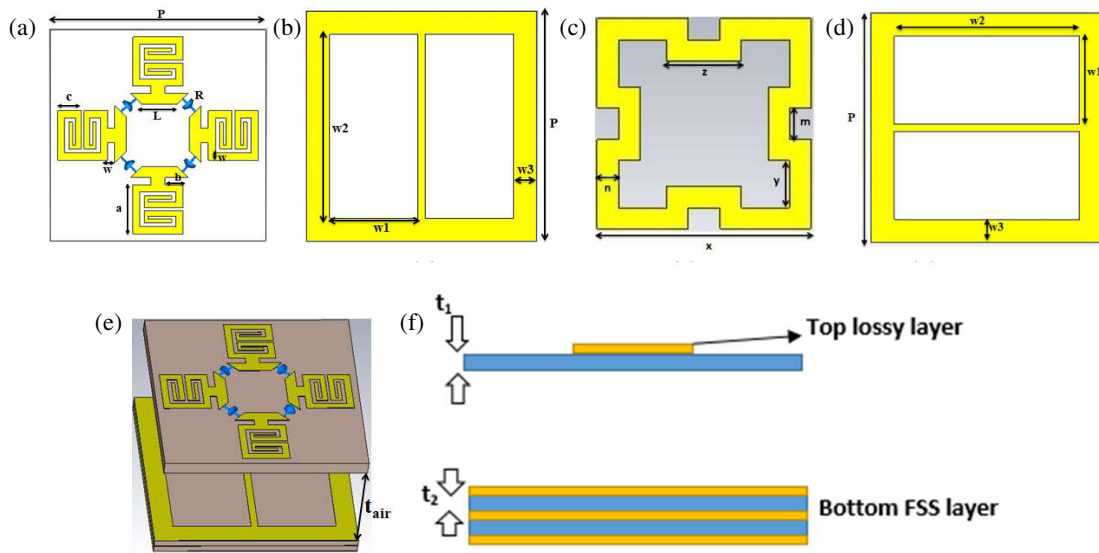
FIGURE 3. Proposed rasorber unit cell structure. (a) Top layer. (b), (c) Middle layers. (d) Bottom layer. (e) Perspective view. (f) Side view of the rasorber.

configuration results in a high impedance at the open end, creating an effective barrier or reflection point for certain frequencies, depending on the length of the transmission line. Hence, it behaves as a parallel resonant circuit, and we get infinite impedance when it resonates. A short-circuited quarter-wave transmission line is a key component in many radio frequency (RF) and microwave designs due to its unique impedance properties. By repeating this structure in all four directions, it is possible to create a system that is insensitive to polarization, providing consistent performance regardless of the orientation of incoming signals. The parallel L_2-C_2 circuit is realized by a modified split ring resonator kept on an FR4 substrate; the finger of the split ring behaves as an inductor, and the coupling between the fingers performs as a capacitor, which is parallel to the inductor. The R_1-L_1-C_1 series circuit is realized by adding four lumped resistors between the modified split ring resonators to get a reflection coefficient below -10 dB in the out-of-band frequency regime. As the top layer is designed for a frequency band, we need to design the bottom layer to resonate at the same frequency band for the transmission window and behave as a ground plane for the out-of-band frequency regime. For this, a parallel L_5-C_5 resonator is kept between two rectangular slots $90°$ to each other in the same plane on the Arlon AD 320A material as shown in Figure 3(c). The inductor (L_5) comes into effect due to the length of the resonator and capacitance due to the gap at four positions, which is parallel to the inductor. To get a narrowband transmission window, we have added two rectangular slots $90°$ to each other, as shown in Figures 3(b), (d), which added two series L_3-C_3 and L_4-C_4 resonators.

The top and bottom layers are separated by foam, which has a refractive index near air. The composite and side view are shown in Figure 3. In this design, lumped resistors with a resistance value of 150 Ohms have been integrated into an FR4 substrate, which possesses a dielectric loss tangent of 0.02 and a permittivity of 4.4. This configuration creates a top lossy layer, contributing to effective out-of-band absorption and a bottom

lossless layer to transmit a range of frequencies. The addition of lumped resistors to the FR4 substrate allows for controlled dissipation of electromagnetic energy, making it ideal for absorbing signals that fall outside the desired transmission range.

The top layer, which contains these lumped resistors, is designed to provide wideband absorption, ensuring that unwanted frequencies are efficiently dampened. This feature is crucial in reducing interference and enhancing the overall performance of the system by minimizing spurious signals.

By carefully adjusting the air gap, the design achieves a balance between out-of-band absorption and in-band transmission. This adjustment allows for precise control over the frequency range where signals are absorbed while a clear transmission band is also maintained for the desired frequencies. The presence of the air gap introduces a level of flexibility, enabling fine-tuning to optimize the system's performance across a wide spectrum.

The combination of the lossy top layer with lumped resistors and adjustable air gap provides a robust mechanism for achieving selective absorption and transmission. This approach is beneficial in applications where it is critical to maintain a specific range of frequencies for transmission while absorbing or blocking out-of-band frequencies.

The optimal parameters of the proposed rasorber are as follows: $P = 15$ mm, $a = 3.5$ mm, $b = 1.25$ mm, $L = 2.42$ mm, $W = 0.5$ mm, $c = 1.65$ mm, $X = 10$ mm, $y = 3$ mm, $z = 3.5$ mm, $m = 1.5$ mm, $n = 1$ mm, $W1 = 5.75$ mm, $w2 = 12$ mm, $w3 = 1.5$ mm, $t_1 = 1$ mm, $t_2 = 0.5$ mm, $t_{air} = 8.0$ mm.

4. DESIGN EVOLUTION

The proposed rasorber comprises two layers. The top resonator passes the in-band signal with a slightly wide response, but the absorption is less in the out-of-band as shown in Figure 4. There are two resonators in the bottom layer. The middle layer trans-
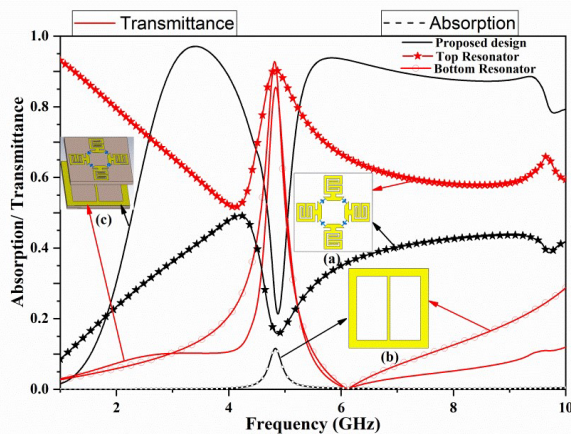
FIGURE 4. Design evolution and performances of the proposed design for (a) only top resonator, (b) only bottom resonator, (c) proposed rasorber.

FIGURE 5. Parametric studies on different values of air thickness.

mits signals when it is in-band and acts as a ground plane when it is out-of-band. To get narrow-band transmission, we added two slots 90° to each other above and below the middle L_5-C_5 resonator.

5. PARAMETRIC STUDY

The parametric studies that are shown below illustrate the performance analysis with varying structural dimension values:

5.1. Effect of Distance between Upper Resonator and Bottom Resonator

The air gap between the top and bottom layers is adjusted to ensure the bottom layer functions as a ground plane for the out-of-band signal and as a band-pass selective filter for the transmission window. During out-of-band operation, the signal is reflected from the bottom layer and re-reflected from the top layer — a process that occurs multiple times to absorb the out-of-band signal and reduce the insertion loss for in-band transmission. To achieve the aforementioned design, we have increased the air space between the top and bottom layers (t_{air}) from 7.0 mm to 9.0 mm. We optimally determined the transmission and reflection coefficients at $t_{air} = 8.0$ mm, as illustrated in Figure 5.

5.2. Effect of Chip Resistor

The chip resistors are responsible for wide-band absorption during out-of-band operation. The values of chip resistors are varied from $R = 100\,\Omega$ to $R = 200\,\Omega$, and the optimum result is found at $R = 150\,\Omega$. We can observe from Figure 6 that chip resistors are responsible for only wide-band absorption in the out-of-band frequency regime; the transmission behavior is unaffected by the chip resistors.

Figure 7 shows the surface current distribution at three different frequencies. Figure 7(b) shows that the surface current near the chip resistors is very low at the transmission window. It means that electromagnetic waves pass through it without any
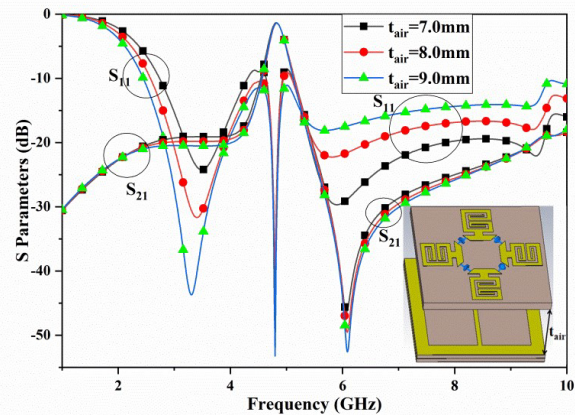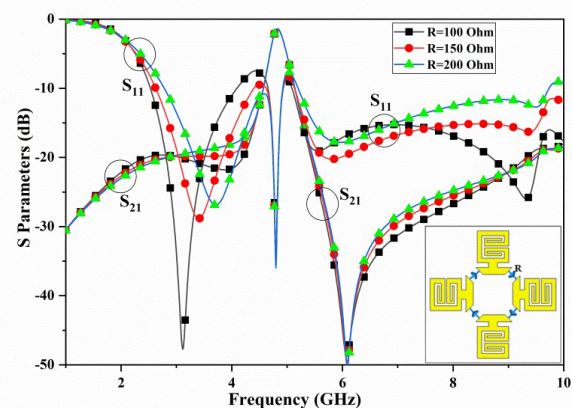
FIGURE 6. Parametric studies on different values of chip resistance.

loss. At the absorption frequency of 3.3 GHz and 6.0 GHz, the surface current distribution is found to be high near the chip resistors as shown in Figures 7(a) and (c). It means that the chip resistors cause losses while the wave passes through them.

6. ABSORPTION/TRANSMISSION PHENOMENA

The proposed rasorber demonstrates its functional range from 2.5 GHz to 9.5 GHz, indicating that within this band, it exhibits the desired behavior of selective transmission and absorption. The proposed design exhibits two distinct absorption bands, each achieving a minimum of 80% absorption, demonstrating its effectiveness in filtering specific frequency ranges. The first absorption band extends from 2.5 GHz to 4.1 GHz, effectively absorbing most of the energy within this lower frequency range. This feature is crucial for reducing noise and interference from lower frequencies, ensuring that the system remains free of unwanted signal reflections and disruptions.

The second absorption band spans from 5.1 GHz to 9.5 GHz, providing robust absorption at higher frequencies. This upper band helps in mitigating interference and maintaining signal integrity in high-frequency applications, contributing to the
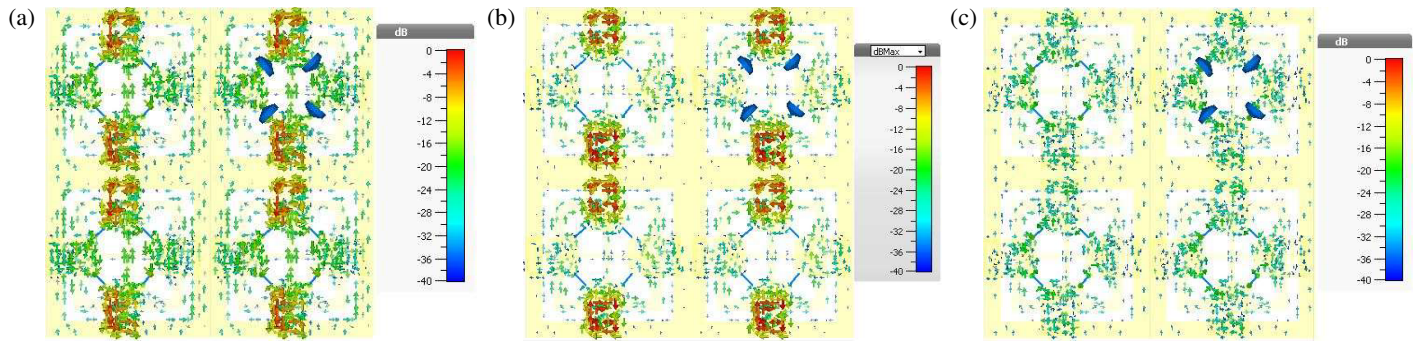
FIGURE 7. Surface current analysis of the proposed design's top layer at (a) 3.3 GHz, (b) 4.8 GHz, (c) 6.0 GHz.
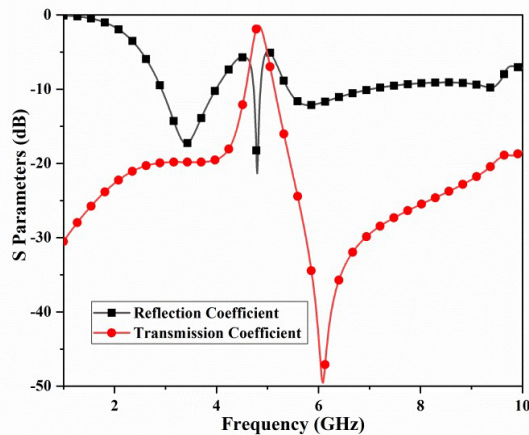
FIGURE 8. Simulated results for the proposed rasorber.
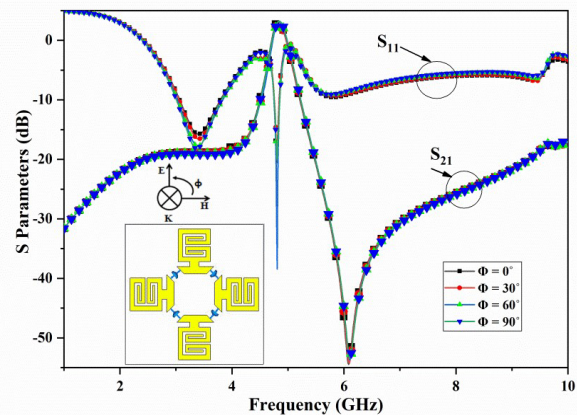
FIGURE 9. Performances for different polarization angles.

system's overall performance by minimizing out-of-band emissions.

Between these two absorption bands, a transmission window is observed near 4.8 GHz. This transmission window allows for selective signal passage through the rasorber, with an insertion loss of just 1.3 dB as shown in Figure 8, indicating minimal signal attenuation. The position of this transmission window is strategically designed to ensure optimal performance within a specific frequency range, providing a clear path for signals while maintaining high absorption on either side. The combination of these absorption bands and transmission window makes the design particularly versatile for applications where a balance between absorption and transmission is required. The high absorption in the defined bands, coupled with a low insertion loss within the transmission window, makes it ideal for a variety of RF and microwave applications, such as communication systems, radar, or electromagnetic compatibility (EMC) solutions.

7. POLARIZATION-INSENSITIVE BEHAVIOR

7.1. Normal Incidence Results

To evaluate the polarization behavior of the proposed rasorber, a test was conducted where the direction of electromagnetic wave propagation remained constant while the orientation of the electric and magnetic fields were rotated, changing the polarization angle (ϕ) incrementally by 30°. This experiment aimed to determine if the rasorber maintained consistent performance despite changes in polarization. As depicted in Figure 9, the simulated results demonstrated that both the reflection and transmission coefficients remained stable across different polarization angles. This outcome is significant as it indicates that the rasorber's behavior is unaffected by polarization variations, confirming its polarization-insensitive characteristics. Such consistency across varying polarization angles is highly desirable in applications where the orientation of incoming waves can vary or is unpredictable. Polarization insensitivity ensures that the rasorber delivers reliable performance, regardless of changes in the polarization of the electromagnetic waves that it interacts with.

7.2. Oblique Incidence Results

Equations (2) and (3) define the reflection coefficients for the TE polarisation ($\Gamma_\perp$) and TM polarisation ($\Gamma_\parallel$) under the oblique incidence angle [19, 20]:

$$\Gamma_\perp(\omega) = \frac{Z(\omega)\cos\theta_i - Z_o\cos\theta_t}{Z(\omega)\cos\theta_i + Z_o\cos\theta_t}, \quad (2)$$

$$\Gamma_\parallel(\omega) = \frac{Z(\omega)\cos\theta_i - Z_o\cos\theta_t}{Z(\omega)\cos\theta_i + Z_o\cos\theta_t}, \quad (3)$$
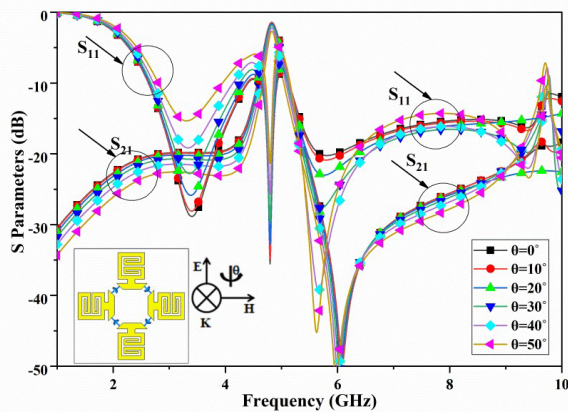
FIGURE 10. Simulated reflection and transmission coefficient of the proposed rasorber for TE Polarization under oblique incidence.

FIGURE 11. Proposed rasorber performances for TM Polarization under different oblique incidence.

where θ_i, θ_t, $Z(\omega)$, and Z_o are the angle of incidence, angle of transmission, impedance of the rasorber, and free space impedance respectively.

The reflection coefficient can change depending on the incident angle, as seen by Eq. (2) and Eq. (3). Figures 10 and 11 show how the reflection and transmission coefficients change for different incident angles (θ_i) when electromagnetic waves with TE and TM polarizations hit the surface.

Figure 10 shows that the reflection coefficient in the upper and lower bands goes down a little as the angle of incidence goes up by 10° steps. However, it stays above 80% for all frequencies up to 50°. The transmission window remains stable up to an incidence angle of 50° with a slight decrease in the insertion loss. In the case of TM polarization, while increasing the angle of incidence, the absorption in the upper band increases, and it remains more than 80% in the lower band also up to 50°. The transmission coefficient is stable up to 50° with little decrease in the insertion loss, which is shown in Figure 11.

8. EQUIVALENT CIRCUIT ANALYSIS

The electrical equivalent circuit model of the proposed rasorber is shown in Figure 12. The equivalent circuit comprises two parts of LC tank circuits. The top layer acts as a lossy layer to provide absorption at the desired bands and at the same time behaves as lossless transparent layer for the transmission window. Thus, this layer constitutes two LC resonance circuits as seen in Figure 12.

The design of top layer is in such a way that a parallel L_2-C_2 circuit can be added in the series to R_1-L_1-C_1 circuit to achieve maximum impedance matching. The top layer band-pass resonance frequency must match the bottom layer passband resonance to get the desired band to be transmitted through the whole structure. The air cavity that separates the top and bottom layers functions as a transmission line (TL2), and the material that forms the top and bottom layers functions as transmission lines (TL1 and TL3). The bottom layer is a cascade of three LC layers to achieve a narrow-band response at the transmission peak. The equivalent circuit of the bottom layer comprises two LC tank circuits, L_3-C_3 and L_4-C_4 due to the upper and
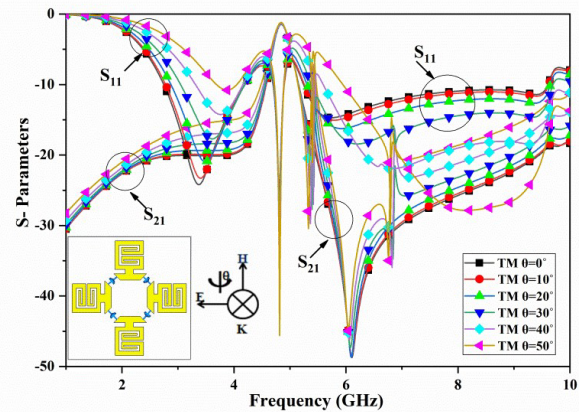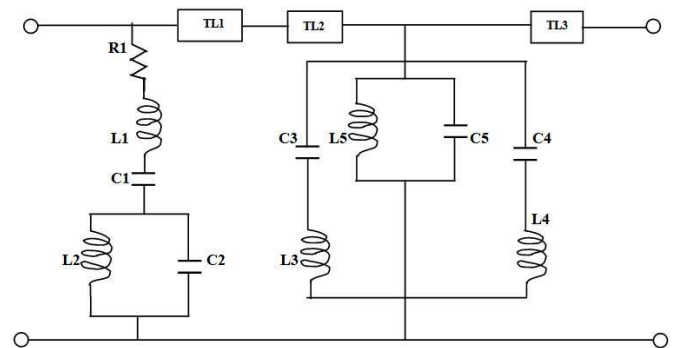
FIGURE 12. Effective equivalent electrical circuit of proposed rasorber.

lower layers of the bottom frequency selective surface and a parallel circuit L_5-C_5, which is due to the band-pass frequency selective layer in middle of the resonator circuit and given in Figure 12. A transmission window is obtained due to parallel LC resonance of the equivalent circuit model, hence overall impedance will be infinity, and signal can easily pass through it.

For the absorption, the impedance of top layer should be matched to the free space impedance, and lower layer will act as a ground plane in the said frequency regime. Based on the electrical equivalent circuit model, the optimized values of the circuit parameters to achieve in-band transmission at 4.8 GHz and two absorption bands (2.5 GHz–4.1 GHz and 5.1 GHz–9.5 GHz) with absorption more than 85% are obtained using Agilent ADS software. The initial set of lumped element values is optimized to ensure that the responses derived from the equivalent circuits and electromagnetic simulation are closely matched.

To achieve the desired reflection and transmission coefficient response, the final values of the lumped elements are as follows: $R1 = 221\,\Omega$, $L1 = 12.20\,\text{nH}$, $C1 = 0.09\,\text{pF}$, $L2 = 2.9\,\text{nH}$, $C2 = 0.36\,\text{pF}$, $L3 = 0.032\,\text{nH}$, $C3 = 0.44\,\text{pF}$, $L4 = 1.37\,\text{nH}$, $C4 = 0.5\,\text{pF}$, $L5 = 0.54\,\text{nH}$, and $C5 = 0.14\,\text{pF}$.

The electrical equivalent model and simulated model are compared in Figure 13. The equivalent circuit analysis and simulated design analysis exhibit a high degree of accord, as we

TABLE 1. Comparison of the proposed Rasorber with already published articles.

References	Design Characteristics & Material	Periodicity (mm × mm/ $\lambda_L \times \lambda_L$)	Transmission Peaks/IL (dB)	Transmission window Bandwidth (-3 dB)	Relative Absorption Bandwidth (lower/Upper absorption band)	Polarization Performances	No. of Lumped elements in one unit cell
[20]	A-T-A, ($\tan\delta = 0.004$) (Expensive)	$11 \times 16.66/0.07 \times 0.11$	9.7 GHz/0.8 dB	40%	83%/36%	Single	2
[21]	A-T-A, $\varepsilon_r = 3$	$24 \times 24/0.22 \times 0.22$	6.3 GHz/0.29 dB	26.2%	91.4%/31.9%	Dual	4
[22]	A-T-A, FR4 ($\tan\delta = 0.025$) (Low cost)	$26 \times 26/0.43 \times 0.43$	7.71 GHz/1.01 dB	102%	18%/9.5%	Dual	12
[23]	A-T-A, F4BM ($\tan\delta = 0.0007$) (Expensive)	$20 \times 20/0.12 \times 0.12$	5.74 GHz/0.25 dB	45%	79.5%/27.3 %	Dual	4
[24]	A-T-A, Rogers 4350B ($\tan\delta = 0.0037$) (Expensive)	$15 \times 15/0.24 \times 0.24$	10 GHz/0.2 dB	32%	79.3%/29%	Dual	4
This Work	A-T-A, FR4 ($\tan\delta = 0.025$) (Low cost)	$15 \times 15/0.12 \times 0.12$	4.80 GHz/1.3 dB	8.3%	44%, 64.52%	Dual	4
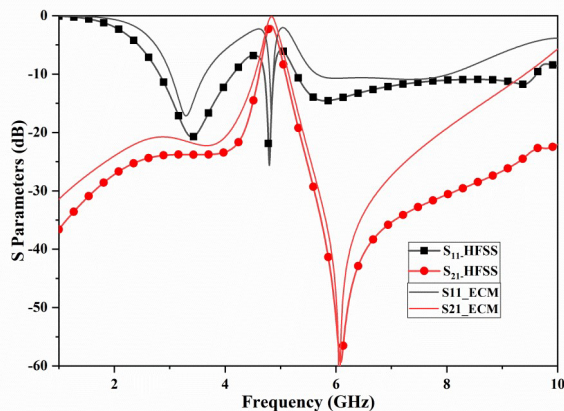
FIGURE 13. Comparison plot with simulated results and ADS circuit model (Circuit parameters).

found. However, the equivalent circuit was unable to produce the precise response. This is because there was no consideration of the mutual coupling between the split ring resonators and adjacent unit cells when the equivalent resistance, inductance, and capacitance were calculated. Additionally, this calculation did not account for the capacitance that results from the top and bottom layer structures, which is why this minor discrepancy is visible.

The performance of the proposed rasorber is compared to that of other existing works in the literature, as illustrated in Table 1. The table illustrates that the proposed rasorber offers a narrow transmission window with a reasonable period-

icity, polarization-insensitivity, stable wide-angle absorption, and a high relative bandwidth in the right side of the absorption spectra. The high periodicity and costly manufacturing cost of certain rasorbers listed in the comparison table enable them to achieve low insertion loss. The proposed rasorber offers a narrow transmission window, less periodicity, and a relatively higher absorption bandwidth on the right side.

9. CONCLUSIONS

This work has demonstrated a novel multilayer rasorber having wide absorption bandwidth of 124% with narrow-band transmission window in the absorption band. This design exhibits a unique combination of in-band transmission and high out-of-band absorption, making it suitable for various applications. The structure comprises two layers: the upper layer is equipped with lumped resistors to facilitate broadband absorption, while the lower layer is carefully engineered to create a narrow transmission window between two distinct absorption bands. To ensure the accuracy of the proposed rasorber, the design was subjected to circuit modeling and other parametric variations. The innovative aspects of this rasorber include its narrow transmission window, high fractional bandwidth, polarization insensitivity, and stable performance across different angles of incidence. Given these features, the proposed rasorber could be employed in various applications, such as Radomes and electromagnetic compatibility solutions, to protect sensitive equipment from unwanted electromagnetic radiation like radio waves and microwaves. Moreover, when being

used as a super-stratum on an antenna, the rasorber can contribute to reduced radar cross-section (RCS), enhancing stealth characteristics. Overall, this dual-polarized rasorber with its unique design and stable behavior across different angles and polarizations offers a versatile solution for applications that require selective frequency transmission and robust absorption, with the added benefit of reducing RCS when being used in antenna systems.

REFERENCES

[1] Costa, F. and A. Monorchio, "A frequency selective radome with wideband absorbing properties," *IEEE Transactions on Antennas and Propagation*, Vol. 60, No. 6, 2740–2747, 2012.

[2] Chen, H., X. Hou, and L. Deng, "Design of frequency-selective surfaces radome for a planar slotted waveguide antenna," *IEEE Antennas and Wireless Propagation Letters*, Vol. 8, 1231–1233, 2009.

[3] Zhou, H., S. Qu, B. Lin, J. Wang, H. Ma, Z. Xu, W. Peng, and P. Bai, "Filter-antenna consisting of conical FSS radome and monopole antenna," *IEEE Transactions on Antennas and Propagation*, Vol. 60, No. 6, 3040–3045, 2012.

[4] Gurrala, P., S. Oren, P. Liu, J. Song, and L. Dong, "Fully conformal square-patch frequency-selective surface toward wearable electromagnetic shielding," *IEEE Antennas and Wireless Propagation Letters*, Vol. 16, 2602–2605, 2017.

[5] Chatterjee, A. and S. K. Parui, "Frequency-dependent directive radiation of monopole-dielectric resonator antenna using a conformal frequency selective surface," *IEEE Transactions on Antennas and Propagation*, Vol. 65, No. 5, 2233–2239, 2017.

[6] Sun, Z., Q. Chen, M. Guo, and Y. Fu, "Low-RCS reflectarray antenna based on frequency selective rasorber," *IEEE Antennas and Wireless Propagation Letters*, Vol. 18, No. 4, 693–697, 2019.

[7] Chen, Q., D. Sang, M. Guo, and Y. Fu, "Frequency-selective rasorber with interabsorption band transparent window and interdigital resonator," *IEEE Transactions on Antennas and Propagation*, Vol. 66, No. 8, 4105–4114, 2018.

[8] Li, B. and Z. Shen, "Wideband 3D frequency selective rasorber," *IEEE Transactions on Antennas and Propagation*, Vol. 62, No. 12, 6536–6541, 2014.

[9] Zhang, H.-B., P.-H. Zhou, H.-P. Lu, Y.-Q. Xu, D.-F. Liang, and L.-J. Deng, "Resistance selection of high impedance surface absorbers for perfect and broadband absorption," *IEEE Transactions on Antennas and Propagation*, Vol. 61, No. 2, 976–979, 2012.

[10] Varuna, A. B., S. Ghosh, and K. V. Srivastava, "An ultra thin polarization insensitive and angularly stable miniaturized frequency selective surface," *Microwave and Optical Technology Letters*, Vol. 58, No. 11, 2713–2717, 2016.

[11] Yi, B., P. Liu, G. Li, and Y. Dong, "Design of miniaturized and ultrathin absorptive/transmissive radome with wideband absorbing property," *Microwave and Optical Technology Letters*, Vol. 58, No. 8, 1870–1875, 2016.

[12] Chen, Q., L. Chen, J. Bai, and Y. Fu, "Design of absorptive frequency selective surface with good transmission at high frequency," *Electronics Letters*, Vol. 51, No. 12, 885–886, 2015.

[13] Kumar, A. and J. Ghosh, "Polarization-independent wideband meta-material absorber based on resistor-loaded hexagonal ring resonators," *Journal of Electromagnetic Waves and Applications*, Vol. 38, No. 2, 264–281, 2024.

[14] Chen, Q., S. Yang, J. Bai, and Y. Fu, "Design of absorptive/transmissive frequency-selective surface based on parallel resonance," *IEEE Transactions on Antennas and Propagation*, Vol. 65, No. 9, 4897–4902, 2017.

[15] Zhang, K., W. Jiang, and S. Gong, "Design bandpass frequency selective surface absorber using LC resonators," *IEEE Antennas and Wireless Propagation Letters*, Vol. 16, 2586–2589, 2017.

[16] Shang, Y., Z. Shen, and S. Xiao, "Frequency-selective rasorber based on square-loop and cross-dipole arrays," *IEEE Transactions on Antennas and Propagation*, Vol. 62, No. 11, 5581–5589, 2014.

[17] Han, Y., W. Che, X. Xiu, W. Yang, and C. Christopoulos, "Switchable low-profile broadband frequency-selective rasorber/absorber based on slot arrays," *IEEE Transactions on Antennas and Propagation*, Vol. 65, No. 12, 6998–7008, 2017.

[18] Yang, C., C.-M. Guo, Y.-X. Wei, and H.-F. Zhang, "Electromagnetic detection design in liquid crystals janus metastructures based on second harmonic generation," *IEEE Transactions on Instrumentation and Measurement*, Vol. 73, 7007811, 2024.

[19] Lei, L., B.-F. Wan, S.-Y. Liao, and H.-F. Zhang, "Broadband asymmetric absorption-transmission and double-band rasorber of electromagnetic waves based on superconductor ceramics metastructures-photonic crystals," *Engineering Science and Technology, An International Journal*, Vol. 57, 101810, 2024.

[20] Sun, Z., Q. Chen, M. Guo, H. Yu, and Y. Fu, "Frequency selective rasorber and reflector with two-sided absorption bands," *IEEE Access*, Vol. 7, 6025–6031, 2018.

[21] Huang, H. and Z. Shen, "Absorptive frequency-selective transmission structure with square-loop hybrid resonator," *IEEE Antennas and Wireless Propagation Letters*, Vol. 16, 3212–3215, 2017.

[22] Hu, Y., S. Liu, X. Kong, and C. Mao, "Low windage resistance frequency-selective rasorber based on windmill-shape coupling line arrays," *Electronics Letters*, Vol. 53, No. 22, 1450–1452, 2017.

[23] Zhang, X., W. Wu, Y. Ma, C. Wang, C. Li, and N. Yuan, "Design dual-polarization frequency selective rasorber using split ring resonators," *IEEE Access*, Vol. 7, 101 139–101 146, 2019.

[24] Chen, Q., D. Sang, M. Guo, and Y. Fu, "Frequency-selective rasorber with interabsorption band transparent window and interdigital resonator," *IEEE Transactions on Antennas and Propagation*, Vol. 66, No. 8, 4105–4114, 2018.

[25] Sen, G., A. Sharma, S. Ghosh, and S. Das, "A wide interabsorption dual-transmission dual-polarized frequency selective rasorber based on SRRs," *Electromagnetics*, Vol. 42, No. 5, 348–358, 2022.

[26] Sen, G., S. Das, and S. Ghosh, "Polarization-insensitive dual-band frequency selective rasorber based on concentric SRRs," in *2020 International Symposium on Antennas and Propagation (ISAP)*, 263–264, Osaka, Japan, 2021.